




## RESEARCH ARTICLE

# The Wayqecha Amazon Cloud Curtain Ecosystem Experiment: A new experimental method to manipulate fog water inputs in terrestrial systems

Daniel B. Metcalfe<sup>1,2</sup>  | Darcy F. Galiano Cabrera<sup>3</sup> | Luis Miguel Alvarez Mayorga<sup>3,†</sup> | Roxana Sacatuma Cruz<sup>3</sup> | Daniela Corrales Alvarez<sup>3</sup> | Blanca Rosa Espinoza Otazu<sup>3</sup> | Walter Huaraca Huasco<sup>3</sup> | Jimmy R. Chambi<sup>3</sup> | Maria E. Ezquerro<sup>3</sup> | Beisit L. Puma Vilca<sup>3,4</sup> | Mark Mulligan<sup>5</sup> | Matthew A. Vadeboncoeur<sup>6</sup> | Heidi Asbjornsen<sup>6,7</sup>  | Paulo R. L. Bittencourt<sup>8</sup> | Aline B. Horwath<sup>3</sup> | David C. Bartholomew<sup>2</sup> 

<sup>1</sup>Department of Physical Geography and Ecosystem Science, Lund University, Lund, Sweden; <sup>2</sup>Department of Ecology and Environmental Science, Umeå University, Umeå, Sweden; <sup>3</sup>Asociación Civil Sin Fines de Lucro Para la Biodiversidad, Investigación y Desarrollo Ambiental en Ecosistemas Tropicales (ABIDA), Cusco, Peru; <sup>4</sup>Department of Geography, King's College London, London, UK; <sup>5</sup>Earth Systems Research Center, University of New Hampshire, Durham, New Hampshire, USA; <sup>6</sup>Department of Natural Resources and the Environment, University of New Hampshire, Durham, New Hampshire, USA; <sup>7</sup>School of Geography, College of Life and Environmental Sciences, University of Exeter, Exeter, UK and <sup>8</sup>Facultad de Ciencias Biológicas, Universidad Nacional de San Antonio Abad del Cusco, Cusco, Peru

## Correspondence

Daniel B. Metcalfe

Email: [dbmetcalfe@gmail.com](mailto:dbmetcalfe@gmail.com)

## Funding information

Royal Geographical Society; Vetenskapsrådet, Grant/Award Number: 2013-06395 and 2019-04779; European Research Council, Grant/Award Number: 682707; Svenska Forskningsrådet Formas, Grant/Award Number: 2015-10002 and 2023-00361; King's College London

Handling Editor: Aaron Ellison

## Abstract

1. Fog makes a significant contribution to the hydrology of a wide range of important terrestrial ecosystems. The amount and frequency of fog immersion are affected by rapid ongoing anthropogenic changes but the impacts of these changes remain relatively poorly understood compared with changes in rainfall.
2. Here, we present the design and performance of a novel experiment to actively manipulate low lying fog abundance in an old-growth tropical montane cloud forest (TMCF) in Peru—the Wayqecha Amazon Cloud Curtain Ecosystem Experiment (WACCEE). The treatment consists of a 30 m high, 40 m wide mesh curtain suspended between two towers and extending down to the ground, and two supplementary curtains orientated diagonally inwards from the top of each tower and secured to the ground upslope. The curtains divert and intercept airborne water droplets in fog moving upslope, thereby depriving a ~420 m<sup>2</sup> patch of forest immediately behind the curtains of this water source. We monitored inside the treatment and a nearby unmodified control plot various metrics of water availability (air humidity, vapour pressure deficit, leaf wetness and soil moisture) and other potentially confounding variables (radiation, air and soil temperature) above and below the forest canopy.

†Deceased.

This is an open access article under the terms of the [Creative Commons Attribution-NonCommercial-NoDerivs](https://creativecommons.org/licenses/by-nc-nd/4.0/) License, which permits use and distribution in any medium, provided the original work is properly cited, the use is non-commercial and no modifications or adaptations are made.

© 2024 The Author(s). *Methods in Ecology and Evolution* published by John Wiley & Sons Ltd on behalf of British Ecological Society.

3. The treatment caused a strong reduction in both air humidity and leaf wetness, and an increase in vapour pressure deficit, above the canopy compared to the control plot. This effect was most pronounced during the nighttime (20:00–05:00). Below-canopy shifts within the treatment were more subtle: relative humidity at 2 m height above the ground was significantly suppressed during the daytime, while soil moisture was apparently elevated. The treatment caused a small but significant increase in air temperature above the canopy but a decrease in temperature in and near the soil, while mixed effects were observed at 2 m height above the ground. Above-canopy radiation was slightly elevated on the treatment relative to the control, particularly during the dry season.
4. Further application of the method in other systems where fog plays a major role in ecosystem processes could improve our understanding of the ecological impacts of this important but understudied climate driver.

#### KEYWORDS

climate change, cloud moisture, drought, large-scale ecosystem manipulation, TCMF, tropical, tropical montane cloud forest

## 1 | INTRODUCTION

A wide range of shifts in precipitation are occurring across the world associated with anthropogenic shifts in land cover and climate change (Caretta et al., 2022; Trenberth, 2011). A predictive understanding of changes in precipitation over space and time, and their ecosystem effects, lags far behind that of temperature for a range of reasons. One major reason is that precipitation events are innately more stochastic (Parsons et al., 2017; Pendergrass et al., 2017). Another aspect is that precipitation occurs in a wide diversity of forms (e.g. rainfall, fog, snow) and regimes (frequency, timing, intensity and lag periods) which create significant additional complexity in understanding the consequences for terrestrial systems (e.g. McCrystall et al., 2021).

To improve understanding of precipitation impacts on terrestrial systems, scientists mainly used observational studies over time (e.g. Carbone et al., 2011; Hereford et al., 2006) and across natural spatial gradients in precipitation (e.g. Austin & Vitousek, 1998; D'Onofrio et al., 2019). For example, Austin and Vitousek (1998) recorded increasing rates of a standardized litter across a ~10-fold change in mean annual precipitation on the island of Hawai'i. These approaches provide important insights into the properties of systems which have equilibrated over extended time periods to differences in precipitation but may provide limited insights into the likely responses of ecosystems as they transition relatively rapidly to ongoing climate change. In addition, these approaches suffer from difficulties inherent to most natural gradient or observational studies in removing the influences of confounding factors which co-vary with the factor of interest (Dunne et al., 2004; Fukami & Wardle, 2005). Increasingly, therefore, scientists have employed a range of methods to artificially simulate shifts in precipitation in the field (Asbjornsen et al., 2018; Beier et al., 2012). However, the overwhelming majority

of these experiments have focused on manipulating mean annual rainfall. For example, two through-fall reduction experiments in the Amazon have dramatically improved the empirical foundation for understanding Amazon drought (Metcalf et al., 2010; Nepstad et al., 2002; Rowland et al., 2015). By comparison, experiments manipulating other precipitation forms and aspects of precipitation regime (e.g. changes in extremes, frequency) are much rarer (Asbjornsen et al., 2018; Knapp, 2024).

One major form of precipitation that remains relatively poorly understood is fog (Bittencourt et al., 2019; Weathers, 1999). Fog constitutes a significant portion of overall precipitation particularly in montane and coastal areas around the world, which together make up a large portion of the earth's surface (Katata, 2014; Moat et al., 2021; Weathers, 1999). Further, new research indicates that fog is also a common feature of many lowland ecosystems (Pohl et al., 2021), providing localized refugia for drought-afflicted organisms (Pohl et al., 2023). In these systems, fog plays a key role in a wide range of important ecosystem processes and properties (Weathers, 1999). Further, plant species within these systems are often specifically adapted to these unusual conditions, and therefore are potentially highly vulnerable to any shifts in fog abundance (Benzing, 1998; Dawson, 1998). Yet, the abundance and frequency of fog is projected to decrease due to surface temperature increases associated with climate shifts and land use change (Antonio Guzmán et al., 2024; Helmer et al., 2019; Still et al., 1999). A range of observational studies have documented negative impacts of fog decline over time on a range of plant and animal groups (Foster, 2001; Pounds et al., 1999). Further, several studies have transplanted plants across sites with different natural levels of fog immersion (Nadkarni & Solano, 2002; Rapp & Silman, 2014) or modified fog abundance/air humidity in a laboratory setting (Carmichael et al., 2020; Limm et al., 2009). These studies generally find that plants adapted to

high fog water inputs tend to suffer negative consequences when exposed to low fog conditions. However, no experiments or technologies have yet been proposed to actively manipulate fog abundance or regime in the field for the purpose of scientific research. This kind of experimental intervention would provide a critical complementary insight to ongoing studies using alternative approaches (e.g. Carmichael et al., 2020; Rapp & Silman, 2014) providing a more rapid and controlled assessment of fog impacts on individual species and for ecosystem processes (Dunne et al., 2004; Fukami & Wardle, 2005).

In this study, we apply and test an approach to manipulate fog abundance over a large area in the field (Figure 1a, Figure S1) drawing inspiration from long-standing techniques used to harvest freshwater from low-lying fog (Verbrugghe & Khan, 2023). Here, we present the results of 2–7 years of monitoring of a range of climatic variables within the fog exclusion treatment plot (hereafter termed 'FE') and an adjacent unmodified control plot (hereafter termed 'CON'). Specifically, we tested how the treatment infrastructure affected metrics of airborne moisture and other relevant aspects of the microclimate (radiation, temperature) above the canopy, below the canopy and near ground level. Further, we discuss opportunities and challenges of adapting the approach to other environments and experimental designs.

## 2 | MATERIALS AND METHODS

### 2.1 | Study site

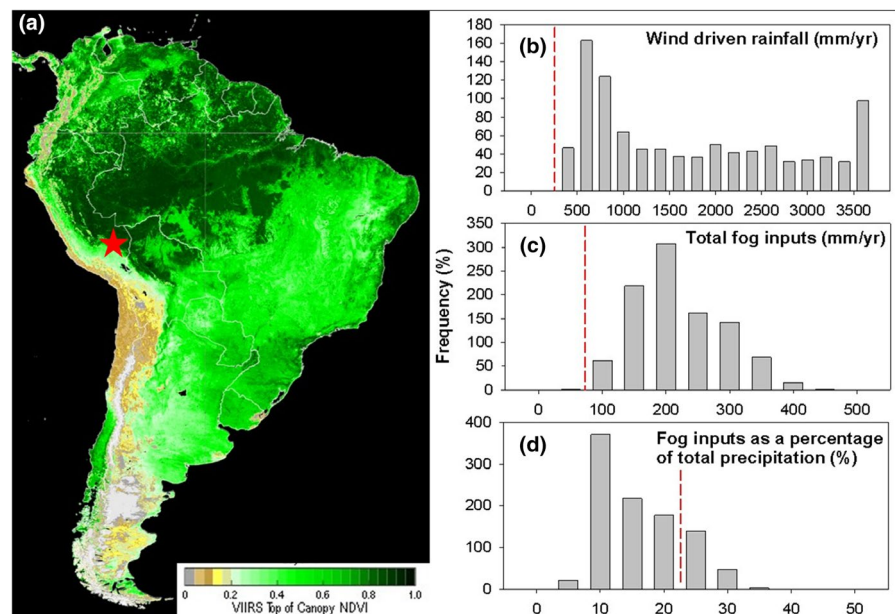
The study site was located within an upper tropical mountain cloud forest c. 1 km from the Wayqecha biological station in the Kosñipata catchment on the eastern (windward) slope of the Andes, Peru (−13.1932°, −71.5883°) around 3000m elevation above sea level. The region is characterized as super humid due to the relative

orientation of prevailing winds and topography, which forms a zone of frequent cloud immersion where cold Andean winds collide with warm, moist air from the Amazonian lowlands (Killeen et al., 2007). Annual precipitation is around 1800mm and daily rainfall occurrence is frequent. Precipitation inputs to the catchment are derived 90.8% from rain and 9.2% from fog, but there is substantial variation in these relative contributions seasonally (Clark et al., 2014). The forest has a closed canopy at around 10–15m height, with a sparse understorey. The tree stems and branches are covered by a large quantity and diversity of epiphytes: bryophytes (mainly liverworts and mosses), ferns, orchids, bromeliads, and the plants of the *Ericaceae* family (Horwath, 2012; Rapp & Silman, 2014).

### 2.2 | Experimental design

In October 2017, one 30-meter-tall aluminium tower was constructed 40m away from an existing 20-m-tall tower that formed part of a canopy walkway at the study site (Figure 2, Figure S1). An additional 10m of tower was added to this existing tower, then a metal cable was suspended between the top of the two towers, and ~3m wide panels of green polyethylene mesh with 3mm aperture diameter (80% shade raschel mesh cloth, Cooperacion Litec SAC, Peru) were strung from a cable to the ground along the whole distance between the towers to form a single continuous curtain (30m high, 40m wide) (Figure 2). This panel was orientated perpendicular to the predominant wind direction to intercept airborne water droplets moving up the forested valley. To support side panels, additional metal cables were also suspended from each tower, oriented at a 60° angle from the main mesh curtain and secured at the other end into the bedrock up-slope of the towers (Figure 2, Figure S1). Mesh panels were also strung from these cables to the ground. Together the main curtain and two side curtains enclosed a triangular patch of forest. Due

**FIGURE 1** Geographic and climatic context of the study site. The red star in panel (a) shows the geographic location of the study site. The panels (b–d) show rainfall and fog regime across the region around the study site, estimated with the WaterWorld hydrological model (Mulligan, 2013). The dashed red line in each panel denotes the specific modelled value for the study site. Background map: NDVI, from NOAA JSTAR MAPPER (<https://www.drought.gov/data-maps-tools/ndvi-greenness-maps>).



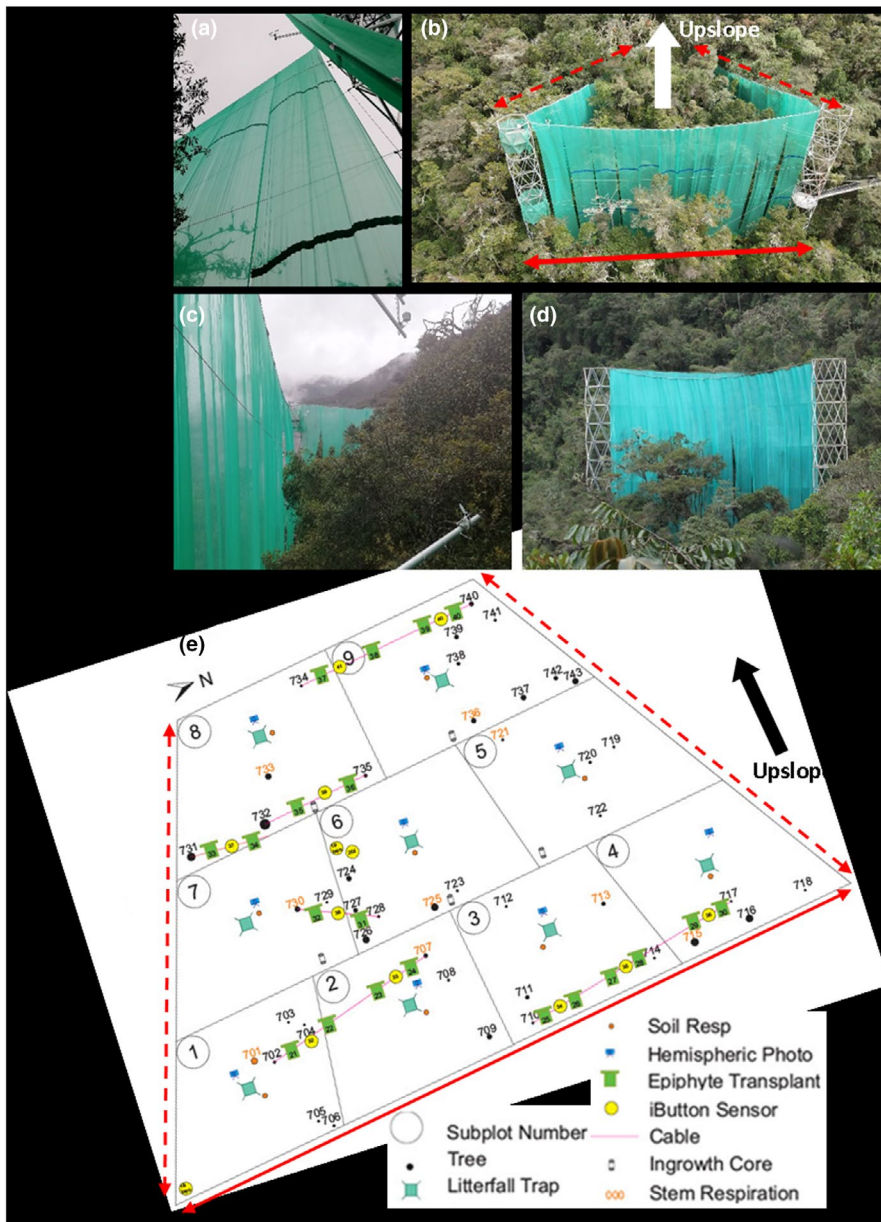


**FIGURE 2** Experimental infrastructure and plot instrumentation. Panels (b, d) show the view upslope directly facing the main curtain. The red lines in (b and e) denote the main curtain perpendicular to the slope (solid line) and the side curtains running diagonally inwards upslope (dashed lines). Note the weather stations visible immediately behind the main curtain above the canopy in panels (a and c). Panel (e) shows the location within the plots of the iButton sensors recording air temperature and humidity within the canopy, the remaining measurements are for ecological monitoring. Panel (b) shows the canopy walkway adjacent to the cloud curtain, and the side curtains running diagonally upslope. The plot shape and spatial arrangement of measurements are identical for the FE and CON plots.

to the steep slope ( $\sim 33^\circ$ ), the emergent canopy (height  $\sim 15$  m) at the upslope corner of the triangular patch overtopped the mesh. Therefore, we only made measurements within the portion of the forest within 20 m from the main mesh panel where the forest canopy was lower than the mesh panels. This  $\sim 420$  m<sup>2</sup> area was designated the FE plot, encompassing 60 trees (DBH  $\geq 10$  cm) from 15 species across 12 families and instrumented with an array of equipment to monitor climatic and ecological variables (Figure 2). The FE plot was open to the sky, to maintain natural light conditions and permit vertical water inputs. Approximately 50 m upslope from the FE plot, the CON plot was established. Both the CON and FE plots were carefully selected to (i) show no signs of human disturbance (e.g. logging, fire) and (ii) have similar species composition, canopy structure and biomass prior to the start of the experiment. Experiment installation and subsequent measurements were covered by Peruvian National Forest and

Wildlife Service permits (RDG 220-2015-SERFOR-DGGSPFFS, RDG 064-2017-SERFOR-DGGSPFFS, RDG 492-2019-MINAGRI-SERFOR-DGGSPFFS, RD-D000010-2022-MIDAGRI-SERFOR-DGGSPFFS-DGSPF).

### 2.3 | Above-canopy meteorology

Three weather stations were installed at the WACCEE experimental site in May 2022, two stations were installed inside the FE plot at approximately 20 m height above the canopy and one station was installed at approximately 20 m height adjacent to the experiment on a third aluminium tower 40 m from the FE plot. The weather stations included a CS320 digital thermopile pyranometer, a HygroVUE5 temperature and relative humidity (RH) sensor enclosed in a RAD06 radiation shield (Campbell Scientific Ltd.,



Loughborough, UK). Data was recorded on a CR1000X measurement and control datalogger and the stations were powered by a SP30 30W solar panel (Campbell Scientific Ltd., Loughborough, UK). Temperature, RH and radiation sensors were calibrated with each other prior to installation. On one station installed inside the WACCEE plot and the station installed adjacent to the experiment, two PHYTOS 31 leaf wetness sensors (METER Group, Munich, Germany) were installed perpendicular to the prevailing wind at a 45° angle. One leaf wetness sensor was installed facing upwards to estimate real leaf wetness conditions capturing both fog and precipitation water. The other leaf wetness sensor was installed facing downwards to mostly capture fog water, although there may be indirect inputs from rainfall via droplet drip and splash.

## 2.4 | Within-canopy meteorology

Hourly air temperature and humidity were sampled with 10 sensors per plot (Hygrochron, Maxim Integrated, San Jose, CA, USA), suspended at 2 m height above the ground. Loggers were shielded to remove any confounding influences from direct radiation and precipitation.

## 2.5 | Soil-level meteorology

Hourly temperature and soil moisture were sampled with five sensors per plot (TMS-4 datalogger, Tomst s.r.o., Michelská, Czech Republic). Temperature was recorded at 3 levels: 15 and 2 cm above the soil surface and 6 cm beneath the soil surface. Moisture was recorded with the time domain transmission method and recorded in raw form as electromagnetic pulses, then converted to volumetric soil moisture with a calibration curve derived for 'Loamy sand A' (Wild et al., 2019) in line with previous work from the study site (Halbritter et al., 2024).

## 2.6 | Hydrological model

WaterWorld is a fully distributed, process-based hydrological model (Mulligan, 2013) that utilizes remotely sensed and globally available datasets. The model requires 145 input maps representing 33 variables over a monthly or diurnal cycle. Baseline climate data at the time of analysis (Oct 2021) was based on long-term climatology from WorldClim (Hijmans et al., 2005). Land use and land cover is represented by three functional vegetation types based at the time on MODIS VCF (Sexton et al., 2013). The model consists of several modules, that is for rainfall distribution (wind-driven rainfall), cloud water interception by vegetation, solar radiation receipt corrected for cloud cover, potential and actual evapotranspiration based on climate and vegetation cover, surface flow and a snow and ice energy balance. Hydrology is simulated for four diurnal time steps representing a mean diurnal cycle

for each of 12 monthly time steps. Water balance is calculated based on incoming wind-driven precipitation, fog and snow inputs minus evapotranspiration. The model has been applied and tested throughout Latin America and parts of tropical Africa and Asia for ET and runoff and wind driven rain and cloud water interception (Bruijnzeel et al., 2011; Ferreira et al., 2019; van Soesbergen & Mulligan, 2014, 2018). In the present study, a baseline simulation was conducted for 1000 randomly chosen points around the study site (between -13 N to -14 S, -72 W to -71 E). The simulations were restricted to pixels with elevations between 1000 and 3700 m with tree cover >40% (which might thus be considered TMCF) for comparability with the study site. From these simulations, the variables wind driven rainfall, total fog inputs and fog inputs as a proportion of total precipitation (rainfall plus fog) were extracted for comparison with the values for the study site.

## 2.7 | Data analysis

Vapour pressure deficit was calculated from temperature and relative humidity by subtracting actual vapour pressure from saturation vapour pressure using Tetens's equation (Tetens, 1930). Since fog only forms once relative air humidity reaches saturation point (100%), we estimated fog formation from relative humidity data by categorizing relative humidity as either equal to 100% or <100%.

To understand differences in climatic conditions between the CON and FE plots, we fitted linear mixed effect models using the lme4 package in the R statistical software (Bates et al., 2015). Each climatic variable was considered as the response variable, with the treatment effect considered as a fixed effect. Date and hour were included as random intercept variables to control for variation in climatic conditions across time, whilst the treatment effect was also included as a random slope effect with hour to test for differences in response with time of day. The maximal model was compared with both a null model and a model without the treatment random slope effect based on the Akaike Information Criterion scores, with the model with the lowest AIC selected following Zuur et al. (2007). To compare between treatments, we fitted equivalent models to all climatic variables with the exception of the categorized relative humidity data where we used a generalized linear mixed model with a binomial error distribution with logit link function to account for the binary nature of the data. Model selection was undertaken in the same manner as the linear mixed effect models described above.

To understand diurnal variation in climatic variables, a generalized additive model was fitted using the mgcv R package (Wood, 2017), with treatment and season included as fixed effects.

To understand how leaf wetness varies with relative humidity, temperature and VPD, we fitted a general linear model with binomial family distribution with treatment and season included as fixed effect variables. Models were fitted using the stats R package (R Core Team, 2023). All analyses were done in R version 4.2.3 (R Core Team, 2023).

### 3 | RESULTS

#### 3.1 | Modelled hydrology

We applied a regional water balance model to estimate the local hydrological context of the study site relative to TMCF across the wider region. The results indicate that the study site experiences relatively low total precipitation (wind driven rainfall plus fog interception), but high proportional contribution of fog to total precipitation, for the region (Figure 1). The forest at the site therefore likely exists close to the regional moisture threshold for TMCF, and appears heavily dependent on fog inputs. These inputs are both from deposition (settling) under low wind speeds and impaction under higher wind speeds. The curtain would intercept impaction by fog moving upslope with the wind, but would not affect the deposition of fog from above.

Estimates of the absolute quantity of water not entering the FE plot due to the mesh curtain are difficult to derive numerically. We applied a basic superposition model (de Dios Rivera, 2011) to estimate a 14% reduction in moisture ingress into the FE plot. Although, this will likely vary substantially according to wind speed and direction, site properties (slope, canopy roughness) and droplet size distribution. This value refers to the quantity of incoming fog water intercepted by the mesh; however, a significant proportion of fog water will be otherwise diverted around the mesh curtains so the actual reduction in the quantity of fog water input immediately behind the curtain is likely higher.

#### 3.2 | Above-canopy relative humidity & vapour pressure deficit

Measurements around 10m above the forest canopy show that the FE treatment causes a significant reduction in overall RH compared to the CON plot (Table 1, Figure 3, Figure S2:  $-4.89 \pm 0.22\%$ ,  $p < 0.001$ ). This RH reduction in the FE plot is greatest at night between 20:00 and 06:00 (Table 1, Figure 3), with a relatively smaller reduction during the daytime (10:00–17:00) (Table 1, Figure 3, Figure S2). This is particularly true during the dry season (June–September) when daytime RH is indistinguishable between plots, whereas there was a smaller but significant reduction in daytime RH on the FE plot compared to the CON in the wet season (October–May; Table 1, Figure 3). These small but significant shifts in RH translate into major plot-level shifts in the amount of time that the air exceeds saturation point to form fog:  $12.7 \pm 1.6\%$  on the CON plot versus  $2.6 \pm 0.4\%$  on the FE plot ( $p < 0.001$ ).

The lower RH on the FE plot, together with the elevated night time air temperature (see below), leads to higher nighttime VPD in the FE plot compared to the CON (Table 1, Figure 3, Figure S2). However, VPD generally remains low, with mean diurnal cycles reaching a max of 0.4 kPa, and an overall maximum VPD across the whole dataset of 1.5 kPa (Figure 3c).

#### 3.3 | Above-canopy leaf wetness

The FE treatment causes strong reductions in leaf wetness (Table 1, Figure 3, Figure S2). Thus, the leaf wetness sensors at ~20m height above the tree canopy in the FE plot remain dry >90% of the time throughout the day in the dry season, reaching near 100% dryness at midday (Table 1, Figure 3), and remaining dry through multiple clear fog events which caused leaf wetting in the CON plot (Figure S2). By contrast, the leaf wetness sensors on the CON plot display more variable wetting and drying cycles, reaching >50% wetness during the night (18:00–06:00) then steadily drying during the day (Table 1, Figure 3). During the wet season, even the FE plot experiences frequent diurnal cycles of leaf wetting. However, this cycle is still much more pronounced in the CON than the FE plot, reaching >80% wetness at night in the CON versus 35% in the FE plot (Table 1, Figure 3). By inverting one of the wetness sensors, we removed any effects of vertical precipitation. These data show broadly the same magnitude and temporal patterns as the non-inverted wetness sensors (Table 1, Figure 3, Figure S2), which indicates that horizontally moving water in fog is driving most of the observed treatment-induced changes in the leaf wetness sensor measurements in the FE plot.

Leaf wetness increased with higher RH, and decreased with increasing temperature and VPD (Figure 4) on both plots. However, leaf wetness declined at much lower temperatures, and much higher RH and VPD levels on the FE plot than the CON, particularly during the dry season (Figure 4). Water droplet formation occurs at higher temperatures (approx. 5°C) in the CON compared with the FE plot.

#### 3.4 | Above-canopy temperature and radiation

The FE treatment slightly but significantly increased air temperature by  $0.45 \pm 0.04^\circ\text{C}$ , potentially due to suppressed evaporative cooling (Table 1, Figure 3, Figure S2). This FE-induced warming effect was minimal during the daytime (09:00–17:00) but higher (1–2°C) during the nighttime (Table 1, Figure 3, Figure S2). The FE treatment increased solar radiation by  $35.73 \pm 4.37 \text{ W}$  ( $p < 0.001$ ) compared to the CON (Table 1, Figure 3), likely due to the decrease in radiation intercepted by the lower levels of fog within the FE plot. This overall difference was particularly driven by a distinct FE treatment-induced radiation increase (~50%) during the dry season (Table 1, Figure 3). By contrast, during the wet season there was a minimal difference in radiation between the FE and CON plots (Table 1, Figure 3).

#### 3.5 | Within-canopy meteorology

Generally, meteorological shifts within the canopy were much less pronounced in the FE plot than above-canopy changes (Table 1, Figure 5). Although, there were significant reductions observed in RH at 2m height above the ground on the FE plot compared to the

**TABLE 1** Mean  $\pm$  standard error for climatic variables in the control (CON) and fog exclusion treatment (FE) plots at midnight and midday in the dry (June–September) and wet (October–May) seasons.

Variable	Canopy position	Midnight						Midday					
		Dry			Wet			Dry			Wet		
		CON	FE	p	CON	FE	p	CON	FE	p	CON	FE	p
Relative humidity (%)	Above	90.20 $\pm$ 0.43	82.87 $\pm$ 0.50	<0.001	97.23 $\pm$ 0.16	91.16 $\pm$ 0.23	<0.001	83.57 $\pm$ 0.38	82.62 $\pm$ 0.36	0.024	91.86 $\pm$ 0.23	89.72 $\pm$ 0.23	<0.001
	Below	96.47 $\pm$ 0.15	97.05 $\pm$ 0.11	0.079	99.36 $\pm$ 0.03	98.94 $\pm$ 0.05	<0.001	92.61 $\pm$ 0.16	90.47 $\pm$ 0.15	<0.001	96.39 $\pm$ 0.06	94.41 $\pm$ 0.08	<0.001
Temperature°C	Above	8.65 $\pm$ 0.05	9.60 $\pm$ 0.04	<0.001	9.69 $\pm$ 0.03	10.59 $\pm$ 0.04	<0.001	13.27 $\pm$ 0.06	12.92 $\pm$ 0.06	<0.001	12.83 $\pm$ 0.05	13.23 $\pm$ 0.05	<0.001
	Below	8.22 $\pm$ 0.02	8.14 $\pm$ 0.10	<0.001	9.60 $\pm$ 0.01	9.74 $\pm$ 0.01	<0.001	12.92 $\pm$ 0.03	12.30 $\pm$ 0.03	<0.001	12.88 $\pm$ 0.02	13.07 $\pm$ 0.02	<0.001
Soil air	Soil air	9.66 $\pm$ 0.02	9.72 $\pm$ 0.02	0.011	10.68 $\pm$ 0.01	10.65 $\pm$ 0.01	0.047	9.81 $\pm$ 0.02	9.46 $\pm$ 0.02	<0.001	10.79 $\pm$ 0.01	10.67 $\pm$ 0.02	<0.001
	Soil surface	10.72 $\pm$ 0.01	10.51 $\pm$ 0.01	<0.001	11.76 $\pm$ 0.01	11.59 $\pm$ 0.01	<0.001	9.52 $\pm$ 0.01	9.53 $\pm$ 0.01	0.672	10.97 $\pm$ 0.01	10.90 $\pm$ 0.01	<0.001
Soil	Soil	11.37 $\pm$ 0.01	10.88 $\pm$ 0.01	<0.001	12.15 $\pm$ 0.01	11.82 $\pm$ 0.01	<0.001	10.30 $\pm$ 0.01	10.13 $\pm$ 0.01	<0.001	11.53 $\pm$ 0.01	11.31 $\pm$ 0.01	<0.001
	Soil	0.11 $\pm$ 0.00	0.21 $\pm$ 0.01	<0.001	0.03 $\pm$ 0.00	0.11 $\pm$ 0.00	<0.001	0.26 $\pm$ 0.01	0.27 $\pm$ 0.01	0.199	0.13 $\pm$ 0.00	0.17 $\pm$ 0.01	<0.001
Vapour pressure deficit (kPa)	Above	0.04 $\pm$ 0.00	0.03 $\pm$ 0.00	0.227	0.01 $\pm$ 0.00	0.01 $\pm$ 0.00	<0.001	0.11 $\pm$ 0.00	0.15 $\pm$ 0.00	<0.001	0.06 $\pm$ 0.00	0.09 $\pm$ 0.00	<0.001
	Below	NA	NA	NA	NA	NA	NA	478.87 $\pm$ 9.99	584.92 $\pm$ 9.81	<0.001	435.77 $\pm$ 7.58	491.15 $\pm$ 7.79	0.021
Solar radiation (W)	Above	0.53 $\pm$ 0.02	0.09 $\pm$ 0.01	<0.001	0.78 $\pm$ 0.01	0.29 $\pm$ 0.01	<0.001	0.08 $\pm$ 0.01	0.03 $\pm$ 0.00	<0.001	0.29 $\pm$ 0.01	0.18 $\pm$ 0.01	<0.001
	Below	NA	NA	NA	NA	NA	NA	0.02 $\pm$ 0.00	0.01 $\pm$ 0.00	0.143	0.06 $\pm$ 0.01	0.08 $\pm$ 0.01	0.186
Upwards facing leaf wetness (proportion)	Above	0.32 $\pm$ 0.02	0.02 $\pm$ 0.00	<0.001	0.61 $\pm$ 0.01	0.14 $\pm$ 0.01	<0.001	0.02 $\pm$ 0.00	0.01 $\pm$ 0.00	0.143	0.06 $\pm$ 0.01	0.08 $\pm$ 0.01	0.186
	Below	NA	NA	NA	NA	NA	NA	0.02 $\pm$ 0.00	0.01 $\pm$ 0.00	0.143	0.06 $\pm$ 0.01	0.08 $\pm$ 0.01	0.186
Downwards facing leaf wetness (proportion)	Above	14.99 $\pm$ 0.09	23.38 $\pm$ 0.13	<0.001	25.08 $\pm$ 0.07	30.02 $\pm$ 0.12	<0.001	15.27 $\pm$ 0.09	23.59 $\pm$ 0.13	<0.001	25.19 $\pm$ 0.07	30.18 $\pm$ 0.12	<0.001
	Below	NA	NA	NA	NA	NA	NA	0.02 $\pm$ 0.00	0.01 $\pm$ 0.00	0.143	0.06 $\pm$ 0.01	0.08 $\pm$ 0.01	0.186
Volumetric water content (%)	Soil	14.99 $\pm$ 0.09	23.38 $\pm$ 0.13	<0.001	25.08 $\pm$ 0.07	30.02 $\pm$ 0.12	<0.001	15.27 $\pm$ 0.09	23.59 $\pm$ 0.13	<0.001	25.19 $\pm$ 0.07	30.18 $\pm$ 0.12	<0.001
	Soil	NA	NA	NA	NA	NA	NA	0.02 $\pm$ 0.00	0.01 $\pm$ 0.00	0.143	0.06 $\pm$ 0.01	0.08 $\pm$ 0.01	0.186

Note: *p*-values are presented for Mann–Whitney *U* tests between the CON and FE plots. Values with significant differences between the CON and FE plot (*p* < 0.05) are highlighted with bold text.

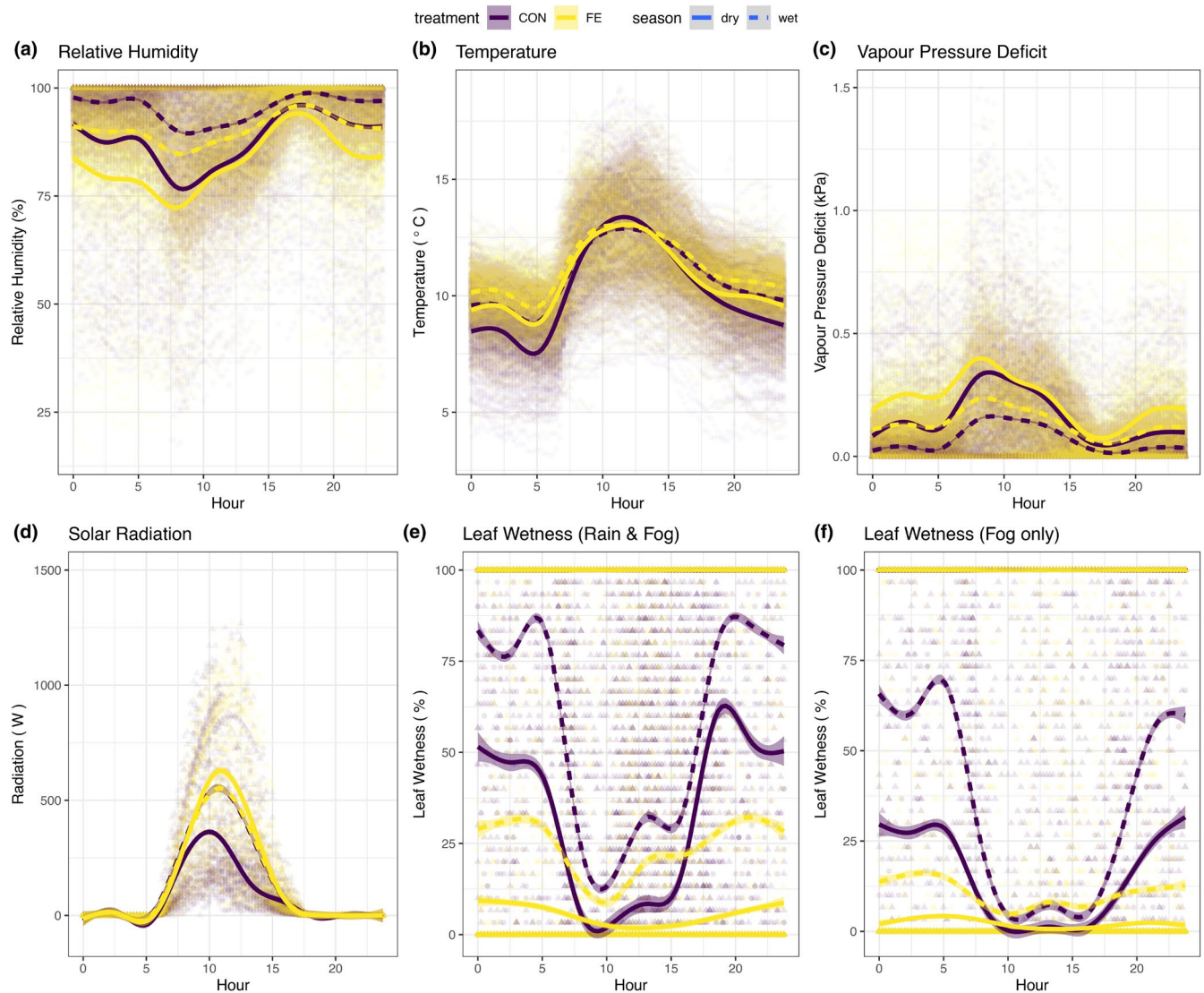


**FIGURE 3** Diurnal cycle of relative humidity (a), air temperature (b), vapour pressure deficit (c), solar radiation (d), upwards facing leaf wetness (e), and downwards facing leaf wetness (f) above the canopy in the control (CON, purple) and fog exclusion (FE, yellow) plots. Data are summaries of records between May 2022–February 2024. Leaf wetness sensors facing upwards and downwards represent moisture intercepted from rain and fog and moisture intercepted from fog only respectively. Relationships are separated by wet season (October–May) and dry season (June–September). Lines represent mean  $\pm$  standard error fitted with generalized additive models.  $n=1$  for the CON plot and 2 for the FE plot.

CON, mainly during the day time (Table 1, Figure 5). Air temperature at 2 m height above the ground was significantly higher on the FE plot than the CON plot during the wet season but lower during the dry season (Table 1, Figure 5). VPD was significantly enhanced under the canopy on the FE plot during the daytime, by around 0.04 kPa (Table 1, Figure 5).

### 3.6 | Meteorology near or in the soil

Physical changes in the soil or near the soil surface were relatively subtle. We identified a small but significant cooling in the FE plot compared to the CON in the soil and close to the soil surface (Table 1, Figure 6). This cooling effect was driven by warming during

15:00–24:00 in the dry season on the CON plot that was apparently suppressed in the FE plot. At other times of the day and year, temperatures at the soil surface and in the soil were very similar (Table 1, Figure 6). Soil moisture was significantly enhanced in the FE plot compared to the CON, and this difference remained fairly stable across diurnal and seasonal cycles (Table 1, Figure 6).

## 4 | DISCUSSION

Ambient cloud dynamics in the CON plot were typical of TMCF: with cloud immersion most common from the late afternoon then through the night until the following morning, particularly during the wet season (Holwerda et al., 2006, Bassiouni et al., 2017,



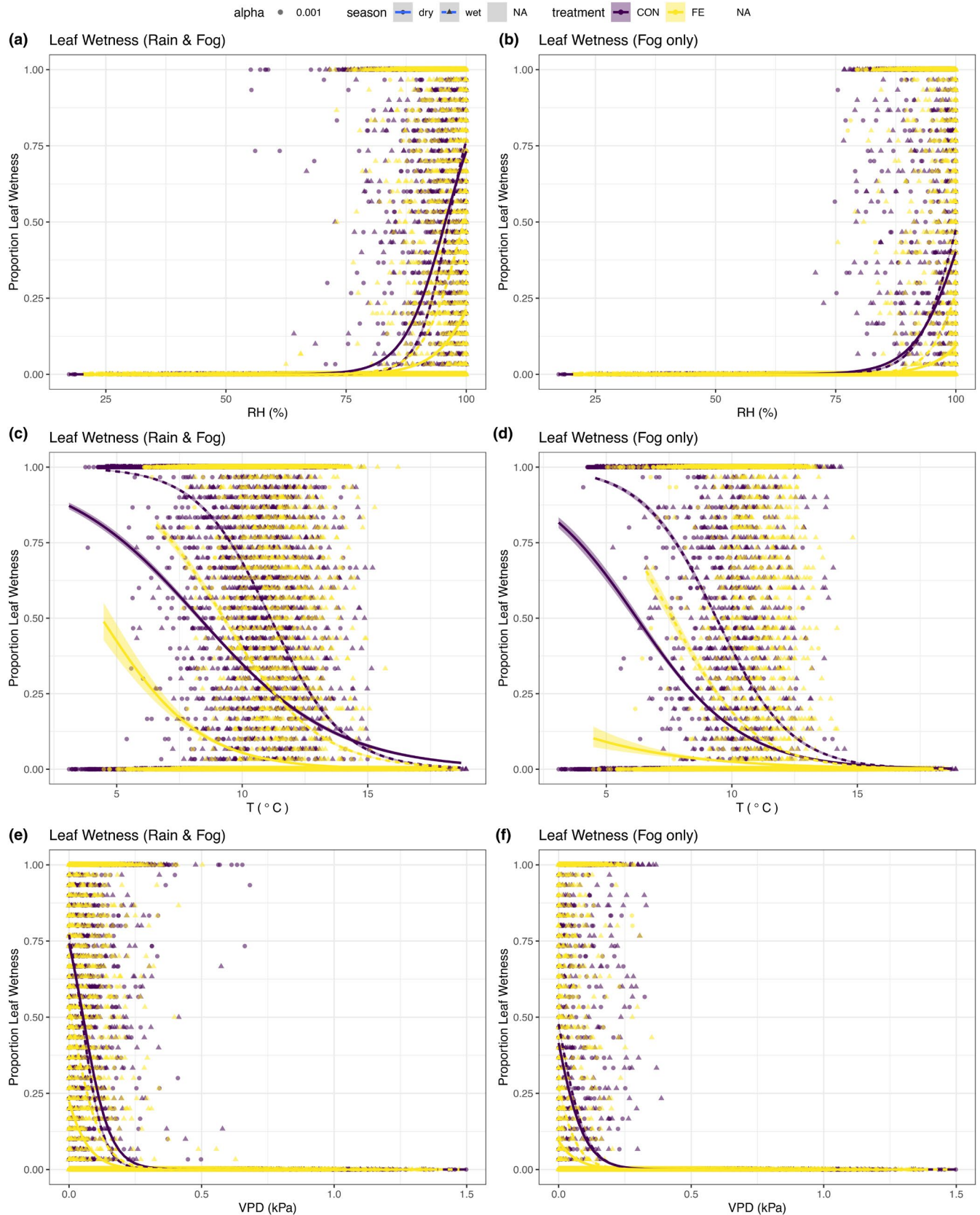


**FIGURE 4** Relationships between leaf wetness and relative humidity (a, b), air temperature (c, d) and vapour pressure deficit (e, f) above the canopy in the control (CON, purple) and fog exclusion treatment (FE, yellow) plots. Data are summaries of records between May 2022–February 2024. Leaf wetness sensors facing upwards and downwards represent moisture intercepted from rain and fog and moisture intercepted from fog only respectively. Relationships are separated by wet season (October–May) and dry season (June–September). Lines represent mean trends fitted with binomial general linear models.  $n = 1$  for the CON plot and 2 for the FE plot.

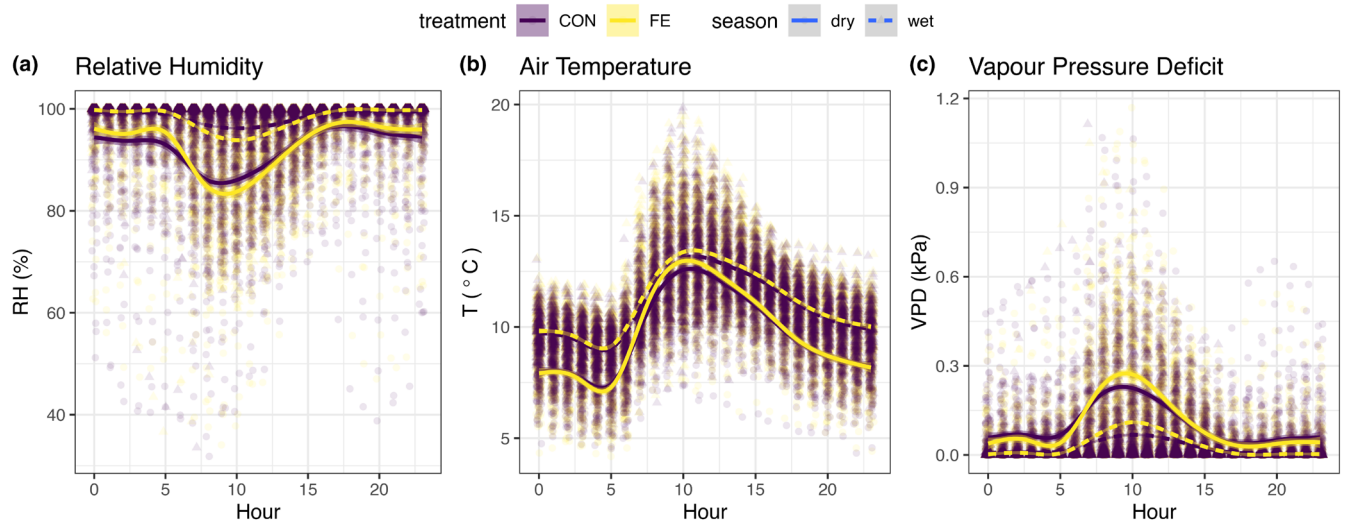


**FIGURE 5** Diurnal cycle of relative humidity (a), air temperature (b) and vapour pressure deficit (c) below the canopy in the control (CON, purple) and fog exclusion treatment (FE, yellow) plots. Data are summaries of records between June 2017–March 2020. Relationships are separated by wet season (October–May) and dry season (June–September). Lines represent mean trends fitted with generalized additive models.  $n=10$  per plot.

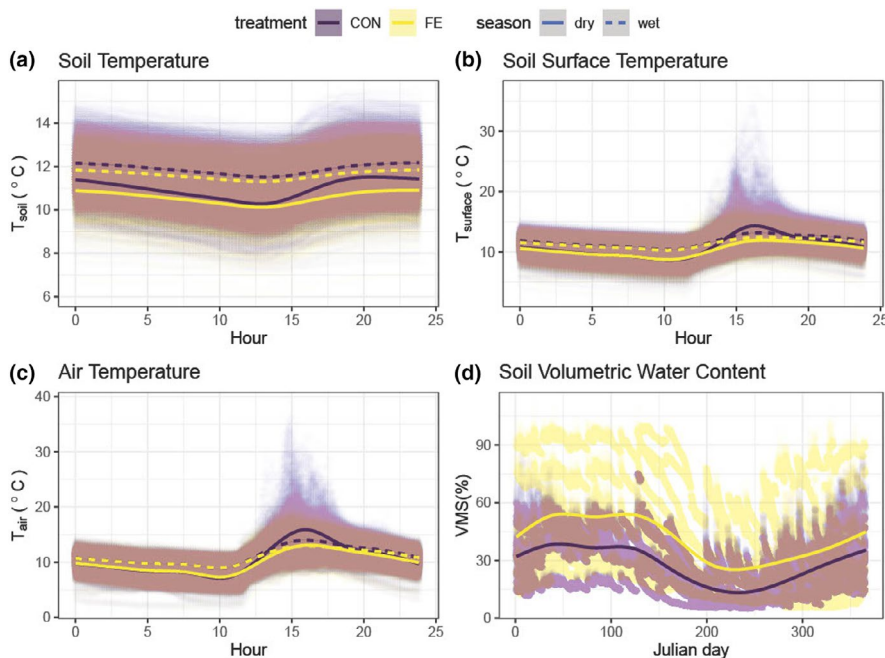


**FIGURE 6** Diurnal cycle of soil and air temperature (a–c) and annual cycle of soil volumetric moisture content (d) in the control (CON, purple) and fog exclusion treatment (FE, yellow) plots. Data are summaries of records between October 2020–November 2023. Temperature was recorded at 6 cm soil depth (a), 2 cm above the soil surface (b) and 15 cm above the soil surface (c). Soil moisture values were integrated over 0–12 cm soil depth. Relationships are separated by wet season (October–May) and dry season (June–September). Lines represent mean trends fitted with generalized additive models.

Bittencourt et al., 2019, but see Li et al., 2022). The WACCEE treatment suppressed this strong diurnal and seasonal signal by reducing laterally moving fog impaction most when ambient fog immersion was greatest (Figure 3). It is not clear what caused the small but significant observed FE treatment-induced shifts in air temperature and radiation, and a large apparent enhancement of soil moisture. The soil moisture differences should be interpreted with caution given the highly localized nature of the measurements and the substantial spatial variability in soil moisture. More widely replicated measurements are required to investigate these differences further. While it is possible that the shifts in air temperature

and radiation are artefacts introduced by the infrastructure, they could also reflect to some extent natural consequences of fog reduction. The decrease in leaf wetting within the FE plot would likely reduce evaporative cooling, which could account for the observed warming within the FE plot. Similarly, it appears likely that a reduction in fog would increase radiation. The fact that the greatest FE-induced increase in radiation occurred during the dry season possibly reflects the relative lack of high-level cloud cover (which was not affected by the FE treatment) during this period, meaning that the relative density of low lying fog (which was affected by the FE treatment) exerted a greater degree of control

over total radiation levels. Alternatively, the likely greater proportion of direct versus diffuse radiation in the dry season could have caused a greater degree of reflection from the nets in the dry season. Further measurements of plant physiology and microclimate within the experiment are underway to distinguish these mechanisms to better understand these overall patterns.

Assessment of the impact of the WACCEE treatment, and comparison with other published results, is hindered by the lack of any single widespread metric used to define fog abundance or frequency. Helmer et al. (2019) classify severe cloud reduction as a reduction in relative humidity greater than 3%. Under a worst case climate change scenario (RCP 8.5), Helmer et al. (2019) project that 34% of Neotropical TMCF will experience these conditions by 2080. The WACCEE infrastructure reduces overall mean annual relative humidity by  $4.9 \pm 0.2\%$ , up to  $\sim 7\%$  in the nighttime, so appears to impose relatively severe levels of fog reduction, which are likely nevertheless to become normal across a significant fraction of neotropical TMCF over this century. Comparatively minor reductions in relative humidity (1.2%–1.5%) have already been linked in other neotropical TMCF to widespread plant and animal community shifts (Bush et al., 2004; Pounds et al., 1999). Therefore, we expect that the FE treatment should be sufficient to stimulate detectable ecological shifts in the study system, even over relatively short periods of time (months to years). The treatment appears successful therefore at providing a relatively rapid insight into ecological responses to likely future climate conditions.

An extensive body of work has accumulated documenting impacts and drivers of fog on terrestrial systems. (Weathers, 1999 and references therein). Increasingly, work across the lowland tropics has documented a wide range of atmospheric and ecosystem interactions mediated by clouds (e.g. Andreae et al., 2004; Blichner et al., 2024; Pöschl et al., 2010; Vilà-Guerau de Arellano et al., 2024). For example, the Amazon Tall Tower Observatory records a wide range of variables along a 325 m tall tower in the central Amazon forest (Andreae et al., 2015), which enables continuous temporal coupling of terrestrial processes with broader meteorological phenomena, including cloud density and frequency (e.g. Vilà-Guerau de Arellano et al., 2024). However, both this work and previous efforts in TMCF and non-tropical systems (Carmichael et al., 2020; Foster, 2001; Limm et al., 2009; Nadkarni & Solano, 2002; Pounds et al., 1999; Rapp & Silman, 2014) have mainly applied models, natural gradients, observations over time and occasionally mesocosms to derive insights. Like any experimental designs and methods, these various approaches suffer from inherent strengths and weaknesses. Some recurring weaknesses are the presence of confounding factors co-varying with the factor of interest (natural gradients & observations over time), the long time required to collect data (observations over time) and the lack of biological realism (models & mesocosms). To partly address these weaknesses, we apply and test a method to experimentally manipulate fog abundance in natural systems. The approach requires construction and maintenance of an experimental infrastructure, so the logistical and financial

challenges can potentially be greater than natural gradients or observations over time. However, unlike these other approaches, the FE treatment can be imposed in a replicated, randomized manner matched with nearby controls to overcome confounding factors. Further, the FE treatment can be imposed near instantaneously and appears, at least in the system and configuration tested here, to cause a reduction in fog abundance that is likely to generate detectable ecological changes relatively rapidly (Bush et al., 2004; Helmer et al., 2019; Pounds et al., 1999). The ability to rapidly construct and remove the treatment could be leveraged to explicitly address scientific questions relating to the timing and frequency of fog events. The spatial scale of the FE treatment, as illustrated in this study, makes it possible to study the integrated effect of fog shifts across multiple interlinked ecological systems in situ, rather than studying individual components or organisms in isolation. However, the basic principle of fog interception by mesh should also function at smaller scales, permitting fog manipulation for individual ecosystem components (e.g. individual microhabitats, plants, or plant organs), which may be beneficial for some scientific questions.

The financial, bureaucratic and logistical challenges inherent in building such an experiment are so highly dependent upon the specifics of the location and scale of the infrastructure that it is difficult to provide useful guidance for building other, similar experiments. The critical component—the mesh which intercepts and diverts airborne water particles—is widely available and relatively cheap ( $\sim$ US\$ 2 per  $m^2$ ). The cost and logistical difficulty is therefore mostly dependent on the scale and spatial arrangement of the physical framework that supports the mesh. In short statured vegetation (e.g. grasses, shrubs, epiphytes), or studies aiming to reduce airborne moisture to individual ecosystem components or plant organs (e.g. leaves, branches) the framework would be relatively small and cheap, and the logistical considerations minimal. Larger frameworks, particularly those located away from roads, will incur much greater costs both from direct fabrication of the framework, installation of the framework in the field and indirectly from building and planning permits. Further, at larger scales the needs for mechanical repair and replacement of the framework and mesh material become more complicated and costly. Although, successful installation of similar structures albeit for a different purpose (to harvest freshwater) in many relatively undeveloped areas in the coastal tropics (Verbrugge & Khan, 2023) indicate that installation and maintenance of even large-scale structures are feasible with limited resources. Prefabricated poles for bearing aerial electricity and telecommunications cables provide one cost-effective option for a larger framework with the necessary load bearing capacity, and can be rapidly installed but require access to the site by large machinery. More remote installations, as detailed in this study, require custom designed and manufactured structures which need to be manually installed piecewise in situ, likely with some anchoring or foundation for stability.

The infrastructure itself appears to introduce some potentially confounding factors (radiation, air temperature), further work is



required to understand if/how these can be minimized. If they arise as indirect products of altered fog, then their inclusion provides a rare opportunity to assess the integrated ecological effects of fog, not solely via altered hydrology but also via indirect shifts in temperature and radiation. An additional important constraint is that the vertical mesh panels mainly only reduce laterally moving impaction fog between 0 and 30m above the ground rather than vertically settling depositional fog. The relative contributions of impaction vs. depositional fog varies widely across the landscape, though typically impaction fog dominates in exposed areas with greater average wind speeds. Modifications to the design to intercept depositional fog could be envisioned (e.g. a horizontal mesh above the canopy), but would likely cause shifts in other climatic factors. We call for further work combining this new manipulative approach with other, more widely applied and tested scientific approaches to derive more robust scientific insights about the current and likely future role of fog in terrestrial ecosystems.

#### AUTHOR CONTRIBUTIONS

Daniel B. Metcalfe conceived of the idea for the experiment, and obtained the funding. Darcy F. Galiano Cabrera, Luis Miguel Alvarez Mayorga, Roxana Sacatuma Cruz, Daniela Corrales Alvarez, Blanca Rosa Espinoza Otazu, Walter Huaraca Huasco, Jimmy R. Chambi, Maria E. Ezquerro, Beisit L. Puma Vilca, Matthew A. Vadeboncoeur, Heidi Asbjornsen, Aline B. Horwath and David C. Bartholomew installed the equipments and collected the data. Daniel B. Metcalfe, David C. Bartholomew, Paulo R. L. Bittencourt and Mark Mulligan analysed the data. Mark Mulligan performed the hydrological modelling. Daniel B. Metcalfe led the writing of the manuscript. All authors contributed critically to the drafts and gave final approval for publication.

#### ACKNOWLEDGEMENTS

We dedicate this study to the memories of construction engineer John Kelson and ecologist Luis Miguel Alvarez Mayorga, whose tireless enthusiasm and resolve was essential for successful installation of the experiment and ecological monitoring within the experiment. Special thanks are due also to Grant Taylor for tower construction, and Fumi Furuya and Renán Valega for transport and other logistics. We are deeply indebted to the Amazon Conservation Association (ACA) or the Asociación para la Conservación de la Cuenca Amazónica (ACCA) for providing access to Wayqecha Research Station, for hosting the experiment on their land, and for assistance with fieldwork logistics and planning. The experiment was funded by the following grants to DBM: Swedish research council for sustainable development (Formas) grants 2023-00361, 2015-10002; Swedish Research Council (Vetenskapsrådet) grants 2019-04779, 2013-06395; European research council consolidator grant ECOHERB 682707. Equipment to MM were funded by [www.FreeStation.org](http://www.FreeStation.org), fieldwork was partly funded by King's College London and the Royal Geographical Society, UK. Abbey Wong, Alice Rigg, Wan Xin Pua, Arnout van Soesbergen and Leo Zurita helped instal equipment.

#### CONFLICT OF INTEREST STATEMENT

The authors declare no conflicts of interest.

#### PEER REVIEW

The peer review history for this article is available at <https://www.webofscience.com/api/gateway/wos/peer-review/10.1111/2041-210X.14483>.

#### DATA AVAILABILITY STATEMENT

Data available via <https://doi.org/10.5061/dryad.s4mw6m9g6> (Metcalfe et al., 2024a) and <https://doi.org/10.5281/zenodo.13727837> (Metcalfe et al., 2024b).

#### ORCID

Daniel B. Metcalfe  <https://orcid.org/0000-0001-8325-9269>

Heidi Asbjornsen  <https://orcid.org/0000-0001-8126-3328>

David C. Bartholomew  <https://orcid.org/0000-0002-8123-1817>

#### REFERENCES

- Andreae, M. O., Acevedo, O. C., Araújo, A., Artaxo, P., Barbosa, C. G. G., Barbosa, H. M. J., Brito, J., Carbone, S., Chi, X., Cintra, B. B. L., da Silva, N. F., Dias, N. L., Dias-Júnior, C. Q., Ditas, F., Ditz, R., Godoi, A. F. L., Godoi, R. H. M., Heimann, M., Hoffmann, T., ... Yáñez-Serrano, A. M. (2015). The Amazon tall tower observatory (ATTO): Overview of pilot measurements on ecosystem ecology, meteorology, trace gases, and aerosols. *Atmospheric Chemistry and Physics*, 15, 10723–10776.
- Andreae, M. O., Rosenfeld, D., Artaxo, P., Costa, A. A., Frank, G. P., Longo, K. M., & Silva-Dias, M. A. F. (2004). Smoking rain clouds over the Amazon. *Science*, 303, 1337–1342.
- Antonio Guzmán, J. Q., Hamann, H. F., & Sánchez-Azofeifa, G. A. (2024). Multi-decadal trends of low-clouds at the tropical montane cloud forests. *Ecological Indicators*, 158, 111599.
- Asbjornsen, H., Campbell, J. L., Jennings, K. A., Vadeboncoeur, M. A., McIntire, C., Templer, P. H., Phillips, R. P., Bauerle, T. L., Dietze, M. C., Frey, S. D., Groffman, P. M., Guerrieri, R., Hanson, P. J., Kelsey, E. P., Knapp, A. K., McDowell, N. G., Meir, P., Novick, K. A., Ollinger, S. V., ... Rustad, L. E. (2018). Guidelines and considerations for designing field experiments simulating precipitation extremes in forest ecosystems. *Methods in Ecology and Evolution*, 9, 2310–2325.
- Austin, A., & Vitousek, P. (1998). Nutrient dynamics on a precipitation gradient in Hawai'i. *Oecologia*, 113, 519–529.
- Bassiouni, M., Scholl, M. A., Torres-Sanchez, A. J., & Murphy, S. F. (2017). A method for quantifying cloud immersion in a tropical mountain forest using time-lapse photography. *Agricultural and Forest Meteorology*, 243, 100–112.
- Bates, D., Mächler, M., Bolker, B., & Walker, S. (2015). Fitting linear mixed-effects models using lme4. *Journal of Statistical Software*, 67, 1–48.
- Beier, C., Beierkuhnlein, C., Wohlgemuth, T., Penuelas, J., Emmett, B., Körner, C., de Boeck, H., Christensen, J. H., Leuzinger, S., Janssens, I. A., & Hansen, K. (2012). Precipitation manipulation experiments—Challenges and recommendations for the future. *Ecology Letters*, 15, 899–911.
- Zuur, A. F., Ieno, E. N., & Smith, G. M. (2007). *Analyzing Ecological Data*. Springer.
- Benzing, D. H. (1998). Vulnerabilities of tropical forests to climate change: The significance of resident epiphytes. *Climate Change*, 39, 519–540.
- Bittencourt, P. R. L., Barros, F. V., Eller, C. B., Müller, C. S., & Oliveira, R. S. (2019). The fog regime in a tropical montane cloud forest in



- Brazil and its effects on water, light and microclimate. *Agricultural and Forest Meteorology*, 265, 359–369.
- Blichner, S. M., Yli-Juuti, T., Mielonen, T., Pöhlker, C., Holopainen, E., Heikkinen, L., Mohr, C., Artaxo, P., Carbone, S., Meller, B. B., Quaresma Dias-Júnior, C., Kulmala, M., Petäjä, T., Scott, C. E., Svenhag, C., Nieradzik, L., Sporre, M., Partridge, D. G., Tovazzi, E., ... Riipinen, I. (2024). Process-evaluation of forest aerosol-cloud-climate feedback shows clear evidence from observations and large uncertainty in models. *Nature Communications*, 15, 969.
- Bruijnzeel, L. A., Mulligan, M., & Scatena, F. N. (2011). Hydrometeorology of tropical montane cloud forests: Emerging patterns. *Hydrological Processes*, 25, 465–498.
- Bush, M. B., Silman, M. R., & Urrego, D. H. (2004). 48,000 years of climate and forest change in a biodiversity hot spot. *Science*, 303, 827–829.
- Carbone, M. S., Still, C. J., Ambrose, A. R., Dawson, T. E., Williams, A. P., Boot, C. M., Schaeffer, S. M., & Schimel, J. P. (2011). Seasonal and episodic moisture controls on plant and microbial contributions to soil respiration. *Oecologia*, 167, 265–278.
- Caretta, M. A., Mukherji, A., Arfanuzzaman, M., Betts, R. A., Gelfan, A., Hirabayashi, Y., Lissner, T. K., Liu, J., Lopez Gunn, E., Morgan, R., Mwanga, S., & Supratid, S. (2022). Water. In H.-O. Pörtner, D. C. Roberts, M. Tignor, E. S. Poloczanska, K. Mintenbeck, A. Alegría, M. Craig, S. Langsdorf, S. Löschke, V. Möller, A. Okem, & B. Rama (Eds.), *Climate change 2022: Impacts, adaptation and vulnerability. Contribution of working group II to the sixth assessment report of the Intergovernmental Panel on Climate Change*. Cambridge University Press.
- Carmichael, M. J., White, J. C., Cory, S. T., Berry, Z. C., & Smith, W. K. (2020). Foliar water uptake of fog confers ecophysiological benefits to four common tree species of southeastern freshwater forested wetlands. *Ecohydrology*, 13, e2240.
- Clark, K. E., Torres, M. A., West, A. J., Hilton, R. G., New, M., Horwath, A. B., Fisher, J. B., Rapp, J. M., Robles Caceres, A., & Malhi, Y. (2014). The hydrological regime of a forested tropical Andean catchment. *Hydrology and Earth System Sciences*, 18, 5377–5397.
- Dawson, T. (1998). Fog in the California redwood forest: Ecosystem inputs and use by plants. *Oecologia*, 117, 476–485.
- de Dios Rivera, J. (2011). Aerodynamic collection efficiency of fog water collectors. *Atmospheric Research*, 102, 335–342.
- D'Onofrio, D., Sweeney, L., von Hardenberg, J., & Baudena, M. (2019). Grass and tree cover responses to intra-seasonal rainfall variability vary along a rainfall gradient in African tropical grassy biomes. *Scientific Reports*, 9, 2334.
- Dunne, J. A., Saleska, S. R., Fischer, M. L., & Harte, J. (2004). Integrating experimental and gradient methods in ecological climate change research. *Ecology*, 85, 904–916.
- Ferreira, P., van Soesbergen, A., Mulligan, M., Freitas, M., & Vale, M. M. (2019). Can forests buffer negative impacts of land-use and climate changes on water ecosystem services? The case of a Brazilian megapropolis. *Science of the Total Environment*, 685, 248–258.
- Foster, P. (2001). The potential negative impacts of global climate change on tropical montane cloud forests. *Earth-Science Reviews*, 55, 73–106.
- Fukami, T., & Wardle, D. A. (2005). Long-term ecological dynamics: Reciprocal insights from natural and anthropogenic gradients. *Proceedings of the Royal Society of London B*, 272, 2105–2115.
- Halbritter, A. H., Vandvik, V., Cotner, S. H., Farfan-Rios, W., Maitner, B. S., Michaletz, S. T., Oliveras Menor, I., Telford, R. J., Ccahuana, A., Cruz, R., Sallo-Bravo, J., Santos-Andrade, P. E., Vilca-Bustamante, L. L., Castorena, M., Chacón-Labela, J., Christiansen, C. T., Duran, S. M., Egelkraut, D. D., Gya, R., ... Enquist, B. J. (2024). Plant trait and vegetation data along a 1314 m elevation gradient with fire history in Puna grasslands, Perú. *Scientific Data*, 21(11), 225.
- Helmer, E. H., Gerson, E. A., Baggett, L. S., Bird, B. J., Ruzycki, T. S., & Voggesser, S. M. (2019). Neotropical cloud forests and paramo to contract and dry from declines in cloud immersion and frost. *PLoS One*, 14, e0213155.
- Hereford, R., Webb, R. H., & Longpré, C. I. (2006). Precipitation history and ecosystem response to multidecadal precipitation variability in the Mojave Desert region, 1893–2001. *Journal of Arid Environments*, 67, 13–34.
- Hijmans, R. J., Cameron, S. E., Parra, J. L., Jones, P. G., & Jarvis, A. (2005). Very high resolution interpolated climate surfaces for global land areas. *International Journal of Climatology*, 25, 1965–1978.
- Holwerda, F., Burkard, R., Eugster, W., Scatena, F. N., Meesters, A. G. C. A., & Bruijnzeel, L. A. (2006). Estimating fog deposition at a Puerto Rican elfin cloud forest site: Comparison of the water budget and eddy covariance methods. *Hydrological Processes*, 20, 2669–2692.
- Horwath, A. B. (2012). *Epiphytic bryophytes as cloud forest indicators: Stable isotopes, biomass and diversity along an altitudinal gradient in Peru* [PhD thesis]. University of Cambridge, Cambridge, UK.
- Katata, G. (2014). Fogwater deposition modeling for terrestrial ecosystems: A review of developments and measurements. *Journal of Geophysical Research-Atmospheres*, 119, 8137–8159.
- Killeen, T. J., Douglas, M., Consiglio, T., Jørgensen, P. M., & Mejia, J. (2007). Dry spots and wet spots in the Andean hotspot. *Journal of Biogeography*, 34, 1357–1373.
- Knapp, A. K., Condon, K. V., Folks, C. C., Sturchio, M. A., Griffin-Nolan, R. J., Kannenberg, S. A., Gill, A. S., Hajek, O. L., Siggers, J. A., & Smith, M. D. (2024). Field experiments have enhanced our understanding of drought impacts on terrestrial ecosystems—But where do we go from here? *Functional Ecology*, 38, 76–97.
- Li, H.-J., Lo, M. H., Juang, J. Y., Wang, J., & Huang, C. Y. (2022). Assessment of spatiotemporal dynamics of diurnal fog occurrence in subtropical montane cloud forests. *Agricultural and Forest Meteorology*, 317, 108899.
- Limm, E. B., Simonin, K. A., Bothman, A. G., & Dawson, T. E. (2009). Foliar water uptake: A common water acquisition strategy for plants of the redwood forest. *Oecologia*, 161, 449–459.
- McCrystall, M. R., Stroeve, J., Serreze, M., Forbes, B. C., & Screen, J. A. (2021). New climate models reveal faster and larger increases in Arctic precipitation than previously projected. *Nature Communications*, 12, 6765.
- Metcalfe, D. B., Meir, P., Aragão, L. E. O. C., Lobo-do-Vale, R., Galbraith, D., Fisher, R. A., Chaves, M. M., Maroco, J. P., da Costa, A. C. L., de Almeida, S. S., Braga, A. P., Gonçalves, P. H. L., de Athaydes, J., da Costa, M., Portela, T. T. B., de Oliveira, A. A. R., Malhi, Y., & Williams, M. (2010). Shifts in plant respiration and carbon use efficiency at a large-scale drought experiment in the eastern Amazon. *New Phytologist*, 187, 608–621.
- Metcalfe, D. B., et al. (2024a). Wayqecha Amazon cloud curtain ecosystem experiment: Climate data and R processing code. *Dryad*. <https://doi.org/10.5061/dryad.s4mw6m9g6>
- Metcalfe, D. B., et al. (2024b). Wayqecha Amazon cloud curtain ecosystem experiment: Climate data and R processing code. *Zenodo*. <https://doi.org/10.5281/zenodo.13727837>
- Moat, J., Orellana-Garcia, A., Tovar, C., Arakaki, M., Arana, C., Cano, A., Faundez, L., Gardner, M., Hechenleitner, P., Hepp, J., Lewis, G., Mamani, J. M., Miyasiro, M., & Whaley, O. Q. (2021). Seeing through the clouds—Mapping desert fog oasis ecosystems using 20 years of MODIS imagery over Peru and Chile. *International Journal of Applied Earth Observation and Geoinformation*, 103, 102468.
- Mulligan, M. (2013). WaterWorld: A self-parameterising, physically based model for application in data-poor but problem-rich environments globally. *Hydrology Research*, 44, 748–769.
- Nadkarni, N. M., & Solano, R. (2002). Potential effects of climate change on canopy communities in a tropical cloud forest: An experimental approach. *Oecologia*, 131, 580–586.
- Nepstad, D. C., Moutinho, P., Dias-Filho, M. B., Davidson, E., Cardinot, G., Markewitz, D., Figueiredo, R., Vianna, N., Chambers, J., Ray, D., Guerreiros, J. B., Lefebvre, P., Sternberg, L., Moreira, M., Barros, L., Ishida, F. Y., Tohlver, I., Belk, E., Kalif, K., & Schwalbe, K. (2002). The effects of partial throughfall exclusion on canopy processes,

- aboveground production, and biogeochemistry of an Amazon forest. *Journal of Geophysical Research*, 107(D20), 8085. <https://doi.org/10.1029/2001JD000360>
- Parsons, L. A., Loope, G. R., Overpeck, J. T., Ault, T. R., Stouffer, R., & Cole, J. E. (2017). Temperature and precipitation variance in CMIP5 simulations and paleoclimate records of the Last Millennium. *Journal of Climate*, 30, 8885–8912.
- Pendergrass, A. G., Knutti, R., Lehner, F., Deser, C., & Sanderson, B. M. (2017). Precipitation variability increases in a warmer climate. *Scientific Reports*, 7, 17966.
- Pohl, M. J., Lehnert, L., Bader, M. Y., Gradstein, S. R., Viehweger, J., & Bendix, J. (2021). A new fog and low stratus retrieval for tropical South America reveals widespread fog in lowland forests. *Remote Sensing of Environment*, 264, 112620.
- Pohl, M. J., Lehnert, L. W., Thies, B., Seeger, K., Berdugo, M. B., Gradstein, S. R., Bader, M. Y., & Bendix, J. (2023). Valleys are a potential refuge for the Amazon lowland forest in the face of increased risk of drought. *Communications Earth & Environment*, 4, 198.
- Pöschl, U., Martin, S. T., Sinha, B., Chen, Q., Gunthe, S. S., Huffman, J. A., Borrmann, S., Farmer, D. K., Garland, R. M., Helas, G., Jimenez, J. L., King, S. M., Manzi, A., Mikhailov, E., Pauliquevis, T., Petters, M. D., Prenni, A. J., Roldin, P., Rose, D., ... Andreae, M. O. (2010). Rainforest aerosols as biogenic nuclei of clouds and precipitation in the Amazon. *Science*, 329, 1513–1516.
- Pounds, J., Fogden, M. P. L., & Campbell, J. H. (1999). Biological response to climate change on a tropical mountain. *Nature*, 398, 611–615.
- R Core Team. (2023). *R: A language and environment for statistical computing*. R Foundation for Statistical Computing.
- Rapp, J. M., & Silman, M. R. (2014). Epiphyte response to drought and experimental warming in an Andean cloud forest. F1000. *Research*, 3, 7. <https://doi.org/10.12688/f1000research.3-7.v2>
- Rowland, L., da Costa, A. C. L., Galbraith, D. R., Oliveira, R. S., Binks, O. J., Oliveira, A. A. R., Pullen, A. M., Doughty, C. E., Metcalfe, D. B., Vasconcelos, S. S., Ferreira, L. V., Malhi, Y., Grace, J., Mencuccini, M., & Meir, P. (2015). Death from drought in tropical forests is triggered by hydraulics not carbon starvation. *Nature*, 528, 119–122.
- Sexton, J. O., Song, X. P., Feng, M., Noojipady, P., Anand, A., Huang, C., Kim, D. H., Collins, K. M., Channan, S., DiMiceli, C., & Townshend, J. R. (2013). Global, 30-m resolution continuous fields of tree cover: Landsat-based rescaling of MODIS vegetation continuous fields with lidar-based estimates of error. *International Journal of Digital Earth*, 6, 427–448.
- Still, C. J., Foster, P. N., & Schneider, S. H. (1999). Simulating the effects of climate change on tropical montane cloud forests. *Nature*, 398, 608–610.
- Tetens, O. (1930). Über einige meteorologische Begriffe. *Zeitschrift für Geophysik*, 6, 297–309.
- Trenberth, K. E. (2011). Changes in precipitation with climate change. *Climate Research*, 47, 123–138.
- van Soesbergen, A., & Mulligan, M. (2018). Potential outcomes of multi-variable climate change on water resources in the Santa Basin, Peru. *International Journal of Water Resources Development*, 34, 150–165.
- van Soesbergen, A. J. J., & Mulligan, M. (2014). Modelling multiple threats to water security in the Peruvian Amazon using the WaterWorld policy support system. *Earth System Dynamics*, 5, 55–65.
- Verbrugge, N., & Khan, A. Z. (2023). Water harvesting through fog collectors: A review of conceptual, experimental and operational aspects. *International Journal of Low-Carbon Technologies*, 18, 392–403.
- Vilà-Guerau de Arellano, J., Hartogensis, O. K., de Boer, H., Moonen, R., González-Armas, R., Janssens, M., Adnew, G. A., Bonell-Fontás, D. J., Botía, S., Jones, S. P., van Asperen, H., Komiya, S., de Feiter, V. S., Rijkers, D., de Haas, S., Machado, L. A. T., Dias-Junior, C. Q., Giovanelli-Haytzmann, G., Valenti, W. I. D., ... Röckmann, T. (2024). CloudRoots-Amazon22: Integrating clouds with photosynthesis by crossing scales. *Bulletin of the American Meteorological Society*, 105, E1275–E1302.
- Weathers, K. C. (1999). The importance of cloud and fog in the maintenance of ecosystems. *Trends in Ecology & Evolution*, 14, 214–215.
- Wild, J., Kopecký, M., Macek, M., Šanda, M., Jankovec, J., & Haase, T. (2019). Climate at ecologically relevant scales: A new temperature and soil moisture logger for long-term microclimate measurement. *Agricultural and Forest Meteorology*, 268, 40–47.
- Wood, S. N. (2017). *Generalized additive models: An introduction with R* (2nd ed.). Chapman and Hall/CRC.

## SUPPORTING INFORMATION

Additional supporting information can be found online in the Supporting Information section at the end of this article.

**Figure S1.** Overview of the design of the experimental infrastructure.

**Figure S2.** Comparison of (a) relative humidity, (b) air temperature, (c) vapour pressure deficit, (d) upwards facing leaf wetness and (e) downwards facing leaf wetness over a 3 day period in the peak dry season (6–8 June 2023) between the control (CON, purple) and treatment (FE, yellow) plots.

**How to cite this article:** Metcalfe, D. B., Galiano Cabrera, D. F., Alvarez Mayorga, L. M., Cruz, R. S., Alvarez, D. C., Otazu, B. R. E., Huaraca Huasco, W., Chambi, J. R., Ezquerra, M. E., Puma Vilca, B. L., Mulligan, M., Vadeboncoeur, M. A., Asbjornsen, H., Bittencourt, P. R. L., Horwath, A. B., & Bartholomew, D. C. (2024). The Wayqecha Amazon Cloud Curtain Ecosystem Experiment: A new experimental method to manipulate fog water inputs in terrestrial systems. *Methods in Ecology and Evolution*, 00, 1–14. <https://doi.org/10.1111/2041-210X.14483>